

Towards athermal Brillouin strain sensing based on heavily Germania-doped core optical fibers

M. Deroh,^{1, a)} T. Sylvestre,¹ J. Chretien,¹ H. Maillotte,¹ B. Kibler,² and J-C. Beugnot¹

¹⁾*Institut FEMTO-ST, UMR 6174 CNRS, Université Bourgogne Franche-Comté, Besançon,*

France

²⁾*Laboratoire Interdisciplinaire Carnot de Bourgogne, UMR 6303 CNRS, Université Bourgogne Franche-Comté, Dijon, France*

(Dated: 15 January 2019)

Owing to their interesting linear and nonlinear optical properties, Germanium-based core optical fibers are being widely used in a wide range of applications ranging from nonlinear optics to optical sensing. We here examine both the strain and temperature coefficients of stimulated Brillouin scattering in heavily-doped core optical fibers with ultra high GeO₂ doping level up to 98-mol %. Our results show that the temperature dependence of the Brillouin gain spectrum becomes almost negligible ($C_T = 0.07 \text{ MHz} \cdot \text{C}^{-1}$) for high doping content, while its Brillouin strain coefficient remains significant ($C_\epsilon = 21.4 \text{ kHz} \cdot \mu\epsilon^{-1}$) compared to that of standard single-mode optical fibers ($C_\epsilon = 48.9 \text{ kHz} \cdot \mu\epsilon^{-1}$). It is further shown that the temperature coefficient tends to zero when removing the fiber coating, indicating that those athermal highly GeO₂-doped-core optical fibers could advantageously be used for Brillouin fiber strain sensing.

I. INTRODUCTION

Stimulated Brillouin scattering (SBS), which relies on the Bragg diffraction of light from a hypersonic beat wave in photo-elastic materials, is a key nonlinear effect for a wide range of photonic applications including high-coherence fiber lasers, narrow-linewidth microwave filters, and fiber optical sensors¹⁻⁴. The latter application has specifically made significant progress in recent years for long-range distributed temperature and strain sensing in structural health monitoring and security asset integrity^{4,5}. The Brillouin-based fiber optical sensors principally exploit the sensitivity of the Brillouin gain spectrum (BGS) in single-mode fibers to temperature and strain^{6,7}. However, because of a linear combination of both temperature and strain, their discrimination still remains a great challenge to date⁸⁻¹¹. Several methods have recently been suggested and demonstrated to overcome this limitation¹²⁻¹⁸. Simultaneous and complete discrimination of strain and temperature was reported by Zou et al. in 2009 by combining both SBS and birefringence measurements in a polarization-maintaining fiber¹². Another method has been later proposed using a multi-core optical fiber where SBS is exploited in both the central core and the outer core of the fiber^{13,14}. In 2012, Dragic et al. made new sapphire-derived all-glass fibers with alumina concentrations, which were found to be athermal, with a Brillouin frequency that was insensitive to changes in temperature. An athermal Brillouin sensor based on these all-glass optical fibers was further demonstrated^{15,16}. More recently, temperature-strain discrimination in distributed optical fiber sensing has been achieved using phase-sensitive optical time-domain reflectometry¹⁷.

Among the wide range of optical fibers available for sensing, GeO₂-based-core optical fibers appear as very attractive candidates due to their **high Brillouin gain, which has been**

recently measured using a pump probe technique¹⁹, and their efficient sensing properties²⁰⁻²³. The BGS dependence on strain and temperature has already been investigated in GeO₂-doped optical fibers and it has been shown that increasing GeO₂ content slightly decreases temperature and strain sensitivity²⁴. However, the GeO₂ core doping level was limited to a moderate amount of 17-mol %.

In this paper, we experimentally investigate Brillouin strain and temperature coefficients in heavily Germanium-doped-core optical fibers with very strong doping level from 53-mol % to 98-mol %²⁰ and we further compare them with standard highly nonlinear (HNLF, 21-mol %) and single-mode fibers (SMF-28, 3.6-mol %). Our measurement results show that the temperature sensing coefficient falls down to almost zero (0.07 MHz/°C) in heavily-doped fibers (98-mol %), while maintaining a large Brillouin gain and a significant strain sensing coefficient of 21.4 kHz/ $\mu\epsilon$. To go further into details, we also show that the temperature sensitivity decreases down to zero by removing the fiber coating, thus revealing that this remarkable athermal behavior is intrinsically related to the Germanium-based core. This is confirmed by a simple analytical model for predicting temperature sensitivity as a function the fiber outer diameter and very good agreement is found with experimental data.

II. EXPERIMENTS

Five different optical fibers with an increasing GeO₂-core doping level were experimentally analyzed and compared for strain and temperature sensing capabilities, including a standard single-mode fiber (SMF-28, 3.6 mol %), a standard highly nonlinear fiber (HNLF-21, 21-mol %) from Sumitomo Electric, and three heavily doped-core fibers from FORC-Photonics with ultra high doping level of 53-mol %, 75-mol %, and 98-mol %, respectively. All the optical and elastic parameters of these fibers are listed in Table 1, which also includes the Brillouin frequency shift (BFS), linewidth, gain,

^{a)}Electronic mail: moise.deroh@femto-st.fr.

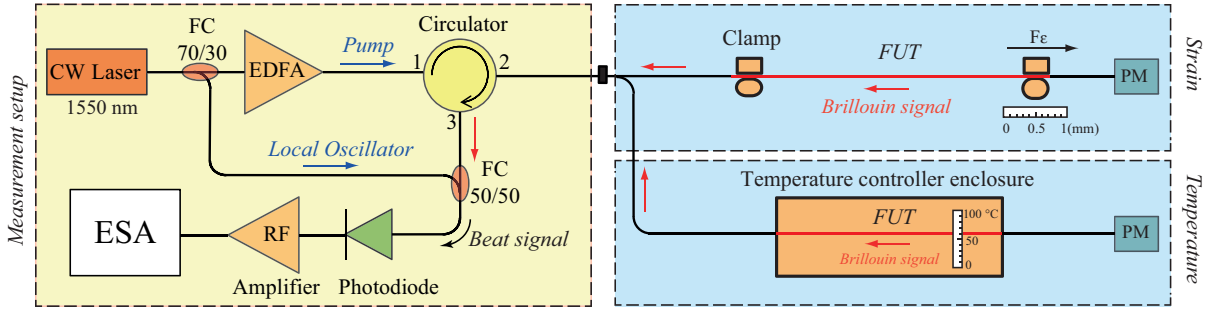


FIG. 1. Scheme of the experimental setup for measuring the Brillouin strain and temperature sensing coefficients by heterodyne detection. EDFA: Erbium-doped fiber amplifier, PM: power meter, ESA: electrical spectrum analyzer, FUT: Fiber under test.

and the critical power threshold, previously reported in Ref.¹⁹. The effective refractive index n_{eff} of the fundamental optical mode and the effective mode area A_{eff} were numerically calculated using a finite element method (COMSOL 5.1 software) based on the opto-geometric parameters of the fibers. From Table 1, we note that increasing the core-doping level significantly reduces both the core diameter and the effective mode area, thus strongly enhancing the Brillouin gain by more than 6. The SBS frequency of our fiber samples without strain at room temperature reduces from 10.85 GHz to 7.703 GHz when increasing the GeO_2 content in the fiber core, while the Brillouin linewidth broadens strongly up to 100 MHz for a 98-mol % doping level.

Figure 1 schematically depicts the experimental setup used for fiber strain and temperature sensing measurements. The experiment is principally based on a highly sensitive optical heterodyne detection of the beat note between a continuous-wave narrow-linewidth (< 10 kHz) laser at 1550 nm and the downshift Brillouin signal coming back from the fiber under test²⁵. The beat frequency is produced by a fast photodetector in the RF domain and the Brillouin gain spectrum is further processed by an electrical spectrum analyzer (ESA) with a high spectral resolution of a few kHz. To measure the strain dependence of the BFS, all optical fibers under test were mechanically fixed using electromagnets over the same length of 1-m only. A force was then applied upon the fibers using motorized translation stages to achieve increasing tensile strain with a sensitivity of $1 \mu\text{m}$ and the resulting BFS was simultaneously measured. For temperature measurements, the fibers were immersed into a thermal water bath filled with demineralized water. The temperature was carefully monitored with an electronic thermometer with a precision of 0.1°C . A power meter was used to precisely monitor the fiber transmission during the measurements.

In optical fibers, the relationship between the BFS (v_B) of the Brillouin gain spectrum and the longitudinal acoustic phonon velocity (V_a) is given by the following formula²⁶:

$$v_B = \frac{2n_{\text{eff}}V_a}{\lambda_p}, \quad (1)$$

where n_{eff} and λ_p are the effective refractive index and the optical pump wavelength, respectively. In germanosilicate-core fibers, the doping level dramatically changes the elastic

properties, in particular the acoustic phonon velocity and the mass density (See Table 1). Correspondingly, the longitudinal acoustic velocity V_a strongly decreases when increasing the core doping level^{24,27,28}. Due to the increase of core doping, the effective refractive index increases as well, while the effective mode area is strongly reduced for single-mode operation, thus giving rise to large nonlinear coefficients and Brillouin gain. For instance, the SBS gain in the HNLF-98 is more than 6 times greater than a standard SMF in spite of **the stronger optical attenuation rate**. The standard linear combination of both strain $\delta\varepsilon$ and temperature δT variations upon BFS can be written as⁸,

$$v_B - v_{B0} = \alpha\delta\varepsilon + \beta\delta T \quad (2)$$

$$\alpha = v_B \left(\frac{1}{n_{\text{eff}}} \frac{\partial n_{\text{eff}}}{\partial \varepsilon} + \frac{1}{V_a} \frac{\partial V_a}{\partial \varepsilon} \right) \quad (3)$$

$$\beta = v_B \left(\frac{1}{n_{\text{eff}}} \frac{\partial n_{\text{eff}}}{\partial T} + \frac{1}{V_a} \frac{\partial V_a}{\partial T} \right) \quad (4)$$

where v_{B0} is the BFS at room temperature. α , β , $\frac{\partial n_{\text{eff}}}{\partial \varepsilon}$, $\frac{\partial n_{\text{eff}}}{\partial T}$ are the strain (in $\text{kHz} \cdot \mu\text{E}^{-1}$), temperature (in $\text{MHz} \cdot ^\circ\text{C}^{-1}$), **elasto-optic and thermo-optic coefficients**, respectively.

III. EXPERIMENTAL RESULTS: BRILLOUIN STRAIN COEFFICIENT

We first measured the backward SBS spectra in all fiber samples at room temperature without any tensile strain applied upon optical fibers. For strain measurements, we limited the elongation up to $7000 \mu\text{E}$ to prevent mechanical reliability issues of our fiber samples. We then applied strain upon only 1-m fiber segment while we use 3-m-long fiber samples. Consequently, two Brillouin resonances are seen in the spectrum, as shown in Figure 2 that illustrates the SBS spectra for an increasing tensile strain from 0 till $7000 \mu\text{E}$ in the HNLF with 98-mol % doping level. The initial RF spectrum measured without applied strain was obtained by using an input pump power of 20 dBm, which is about 15 dB below the Brillouin threshold. The SBS spectrum has a main single peak located

at 7.703 GHz with a linewidth of 98.5 MHz. The impact of tensile strain is clearly noticeable from 2000 $\mu\epsilon$ with a resulting continuous shift of the SBS frequency up to 7.85 GHz related to strain applied upon the 1-m-long fiber segment. Figure 3 (a) shows the resulting strain dependence of the BFS of the five germano-silicate fibers as a function of the GeO_2 doping level.

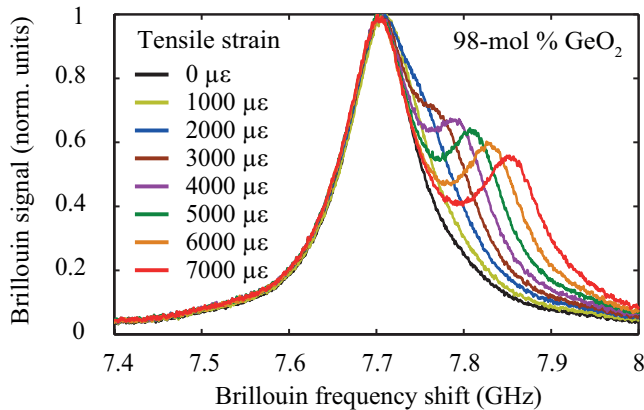


FIG. 2. Experimental backscattering Brillouin spectra for 98-mol % GeO_2 core doping for an increasing tensile strain from 0 till 7000 $\mu\epsilon$. Resolution bandwidth (RBW) is 100 kHz.

In all cases, we observe that the BFS linearly increases linear with the tensile strain, as in standard silica optical fibers¹⁰. The germanosilicate-core indeed modifies significantly the fiber acoustic properties such as the acoustic phonon velocity and the Young modulus, leading to strong decrease of both the BFS and the SBS strain coefficient, as shown in Fig. 3(b) with a quadratic decrease of the strain coefficient as a function of GeO_2 content. At low doping level, it has been reported that the strain sensitivity linearly depends of GeO_2 core content²⁴. However, this dependence drastically changes for heavily-doped fibers, since we observe a quadratic behavior of SBS strain coefficient decreasing down to 21.4 $\text{kHz}/\mu\epsilon$ for ultra-high doping level of 98-mol %.

IV. EXPERIMENTAL RESULTS: BRILLOUIN TEMPERATURE COEFFICIENT

Temperature gradient from 20°C to 68°C was afterwards applied upon the fibers without any tensile strain. Figure 4 shows for instance two Brillouin spectra measured in the 98-mol % GeO_2 content fiber and recorded for the lowest and highest temperature values. The plots in Fig. 4 show that the Brillouin gain spectrum does not dramatically change and the BFS only slightly increases from 7.703 GHz (20°C) to 7.706 GHz (68°C). This can be related to the high GeO_2 core doping level that makes the fiber insensitive to temperature. We can also observe that the Brillouin linewidth (99.7 MHz at 20°C, blue line and 93.9 MHz at 68°C, red line) slightly narrows due to the temperature increase. **This is related with the fact that increasing the temperature enlarges the acoustic**

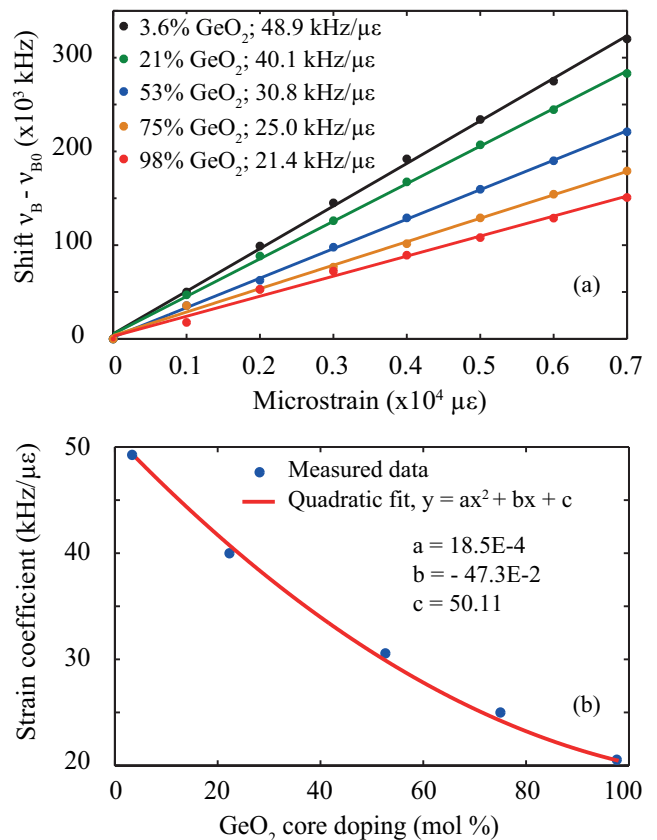


FIG. 3. (a) Brillouin frequency shift versus micro strain applied on the five germanosilicate fibers with varying doping level; (b) Strain coefficient versus GeO_2 -core doping level.

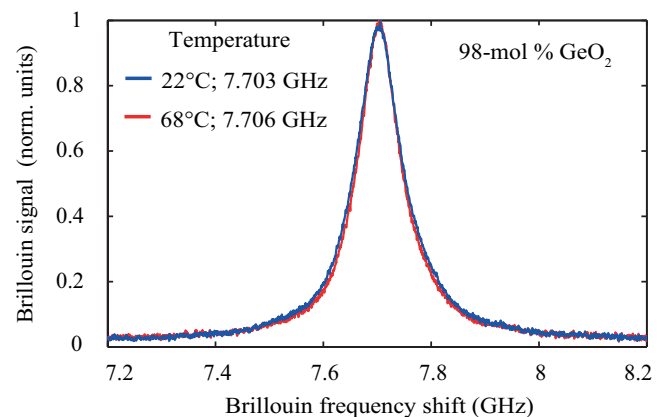


FIG. 4. Experimental backscattering Brillouin spectra measured at two different temperatures for the fiber with 98-mol % doping level.

phonon lifetime. The gain spectral narrowing is of about 1 MHz per 10°C, which is in very good agreement with previous observations²³. In Fig. 5 (a), we confirm the linear dependence of BFS as a function of temperature in all the fibers, from 3.6 mol % to 98-mol % GeO_2 content. Figure 5(b) shows the variation of Brillouin temperature coefficient as a

TABLE I. Optical and sensing parameters of the five different GeO₂-doped-core optical fibers under test.

Fiber parameters	Units	SMF-28	HNLf-21	HNLf-53	HNLf-75	HNLf-98
Core GeO ₂ content	mol %	3.6	21	53	75	98
Core diameter, ϕ	μm	8.2	5	4.7	2.3	2
Fiber losses@1.55 μm , α	dB.km ⁻¹	0.21	0.8	10	20	200
Effective area@1.55 μm , A_{eff}	μm^2	78.3	12.8	11	4.7	3.5
Refractive index@1.55 μm , n	-	1.449	1.489	1.535	1.567	1.601
Effective index@1.55 μm , n_{eff}	-	1.446	1.467	1.509	1.519	1.531
Acoustic Velocity, V_L	m.s ⁻¹	5960	5059	4480	4139	3898
Mass density, ρ	kg.m ⁻³	2210	2507	2960	3271	3596
Brillouin frequency, ν_B	GHz	10.845	9.648	8.726	8.067	7.703
Brillouin linewidth, $\Delta\nu_B$	MHz	28	55	89	94	98
Brillouin threshold, P_{th} , (for 3m length)	dBm	44.8	40.1	39.6	35.8	34.6
Brillouin gain, $\frac{g_B}{A_{\text{eff}}}$	W ⁻¹ .m ⁻¹	0.23	0.38	0.92	1.15	1.62
Normalized SBS gain	dB.m ⁻¹ .W ⁻¹	1	1.7	4	4.9	6.6
Strain coefficient	kHz. $\mu\epsilon$ ⁻¹	48.9	40.1	30.8	25.0	21.4
Temperature coefficient	MHz. $^\circ\text{C}^{-1}$	1.09	0.86	0.48	0.21	0.07

function of GeO₂ core doping level. It nonlinearly decreases from 1.09 MHz/ $^\circ\text{C}$ (SMF, 3.6-mol %) down to 0.07 MHz/ $^\circ\text{C}$ (HNLf, 98-mol %). For ultra-high GeO₂ doping level, the temperature coefficient is 15 times smaller than that of standard silica optical fibers, whereas the strain coefficient is only 2 times smaller than SMF-28. For the temperature variation considered here, ranging from 20 $^\circ\text{C}$ to 68 $^\circ\text{C}$, the temperature coefficient does not really change.

These properties could be very useful to efficiently discriminate the temperature and the strain effects in optical fiber sensors. We note however that the increasing attenuation losses in such heavily GeO₂-doped-core optical fibers (up to 200 dB.km⁻¹) could limit the sensing range to a few meters despite the higher Brillouin gain compared to standard fibers.

Finally, we removed the fiber coating using acetone in order to better understand the athermal behavior of heavily GeO₂ doped core fibers. In standard single-mode fibers (SMF-28), the fiber coating indeed modifies the SBS temperature coefficient by a small amount, as reported in Refs.^{29,30}. The SBS temperature sensitivity of the fiber with 98-mol % GeO₂ content is reported on Fig. 5 (b) (green dot). We observe that the temperature sensitivity (- 0.02 MHz. $^\circ\text{C}^{-1}$) is very close to 0 MHz. $^\circ\text{C}^{-1}$ without the polymer coating, thus proving that a remarkable athermal behavior is only related to ultra-high GeO₂ doping level of the fiber core. More importantly, by monitoring the optical coating thickness of the fibers, we could modify coating thermal strain effect on SBS temperature measurements. Consequently, a perfectly athermal fiber could be readily developed³¹. This is shown in Fig. 6 both experimentally in (blue dots) and and theoretically (red curve). For theory, we used the following analytical equations according to Refs.^{29,30}

$$\frac{\partial \nu_B}{\partial T} = \left(\frac{\partial \nu_B}{\partial T}\right)_{\text{bare fiber}} + \left(\frac{\partial \nu_B}{\partial \epsilon} * \frac{\partial \epsilon}{\partial T}\right)_{\text{coating}} \quad (5)$$

$$\left(\frac{\partial \epsilon}{\partial T}\right)_{\text{coating}} = \frac{E_2 A_2 (\alpha_2 - \alpha_1)}{E_2 A_2 + E_1 A_1} \quad (6)$$

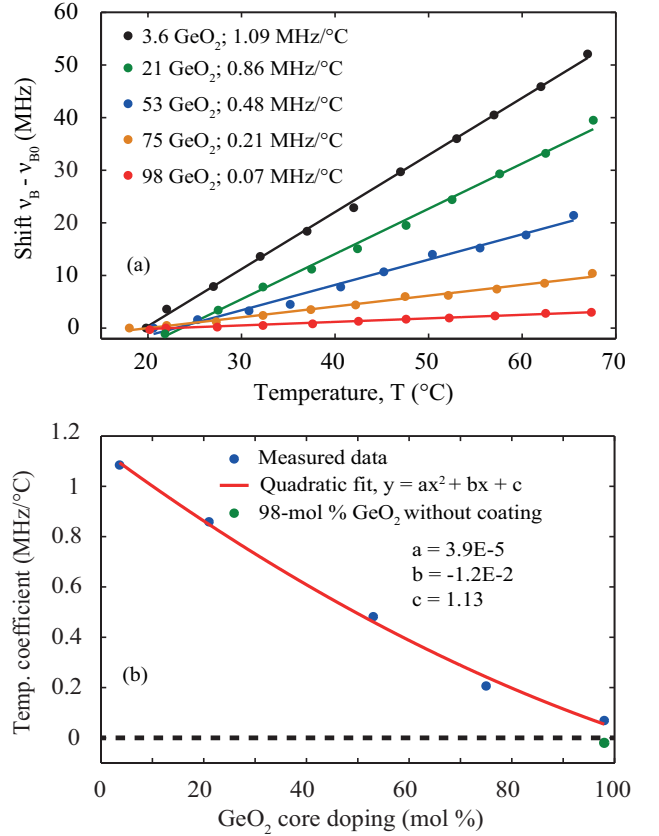


FIG. 5. (a) Brillouin frequency shift versus the temperature increase in five different fibers; (b) SBS temperature coefficient versus GeO₂-core doping levels.

where $\frac{\partial \nu_B}{\partial T}$, $\frac{\partial \nu_B}{\partial \epsilon}$ and $\frac{\partial \epsilon}{\partial T}$ are the strain (in kHz. $\mu\epsilon$ ⁻¹), temperature (in MHz. $^\circ\text{C}^{-1}$) coefficients and the thermal strain induced by the coating material upon the fiber bare (in $^\circ\text{C}^{-1}$), respectively. $E_{1,2}(7.2 \times 10^{10} \text{ n.m}^{-2}, 0.8 \times 10^{10} \text{ n.m}^{-2})$,

$A_{1,2}$ (in m^2) and $\alpha_{1,2}$ ($5.5 \times 10^{-7} C^{-1}$, $1.5 \times 10^{-4} C^{-1}$) are the Young's modulus, cross-sectional areas, and the thermal expansion coefficients of both fiber bare and coating material, respectively³². From Eqs. 5 and 6, we plotted in Fig. 6 the evolution of the Brillouin temperature sensitivity (in $MHz \cdot ^\circ C^{-1}$) of the heavily 98-mol % GeO_2 content optical fiber as a function of the overall outer diameter of the fiber (in μm). Our results show that a fully athermal optical fiber could be achieved by reducing the coating thickness down up to 155 μm .

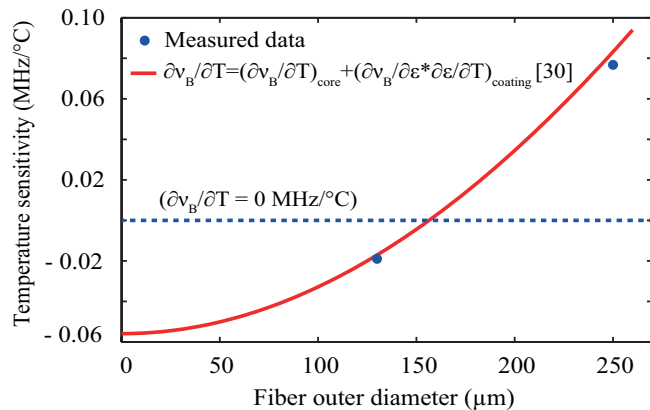


FIG. 6. Temperature sensitivity as a function of the overall fiber outer diameter. Experimental data (blue dots) versus theory (red curve).

V. CONCLUSION

To conclude, we have experimentally investigated the temperature and tensile strain sensing potential of several heavily-doped Germania-core optical fibers. Our results have demonstrated that the use of doping levels as high as 98-mol % allows for an almost complete elimination of the thermal coefficient, with only a small reduction of the strain coefficient, thus enabling strain sensing possibilities with no temperature crosstalk. It was further shown that a completely athermal optical fiber would require to reduce the coating diameter down to 155 μm . Furthermore, in contrast to previous observations, at low concentrations doses, showing a linear decrease of the strain coefficient as a function of the GeO_2 doping level, our results demonstrated that, at high concentration levels, the coefficient decreases with a quadratic dependence.

FUNDING

This work has received funding from by the French National Research Agency under grant agreements ANR-17-EURE-0002, ANR-16-CE24-0010-03, and ANR-15-IDEX-0003. Moise Deroh thanks the Conseil Régional de Bourgogne Franche-Comté for student scholarship.

REFERENCES

- ¹A. Kobyakov, M. Sauer, and D. Chowdhury, "Stimulated Brillouin scattering in optical fibers," *Adv. Opt. Photonics* **2**, 1–59 (2010).
- ²J. Li, H. Lee, T. Chen, and K. J. Vahala, "Characterization of a high coherence, Brillouin microcavity laser on silicon," *Opt. Express* **20**, 20170–20180 (2012).
- ³D. Marpaung, C. Roeloffzen, R. Heideman, A. Leinse, S. Sales, and J. Capmany, "Integrated microwave photonics," *Laser & Photonics Rev.* **7**, 506–538 (2013).
- ⁴C. A. Galindez-Jamioy and J. M. Lopez-Higuera, "Brillouin distributed fiber sensors: an overview and applications," *J. Sens.* **204121** (2012).
- ⁵P. Dragic and J. Ballato, "A Brief Review of Specialty Optical Fibers for Brillouin-Scattering-Based Distributed Sensors," *Appl. Sci.* **8**, 1996 (2018).
- ⁶T. Horiguchi, K. Shimizu, T. Kurashima, M. Tateda, and Y. Koyamada, "Development of a distributed sensing technique using Brillouin scattering," *J. Light. Technol.* **13**, 1296–1302 (1995).
- ⁷M. Niklès, L. Thévenaz, and P. A. Robert, "Simple distributed fiber sensor based on Brillouin gain spectrum analysis," *Opt. Lett.* **21**, 758–760 (1996).
- ⁸T. R. Parker, M. Farhadiroushan, V. A. Handerek, and A. J. Rogers, "Temperature and strain dependence of the power level and frequency of spontaneous Brillouin scattering in optical fibers," *Opt. Lett.* **22**, 787–789 (1997).
- ⁹Y. Mizuno and K. Nakamura, "Potential of Brillouin scattering in polymer optical fiber for strain-insensitive high-accuracy temperature sensing," *Opt. Lett.* **35**, 3985–3987 (2010).
- ¹⁰M. N. Alahbabi, Y. T. Cho, and T. P. Newson, "Simultaneous temperature and strain measurement with combined spontaneous Raman and Brillouin scattering," *Opt. Lett.* **30**, 1276–1278 (2005).
- ¹¹C. C. Lee, P. W. Chiang, and S. Chi, "Utilization of a dispersion-shifted fiber for simultaneous measurement of distributed strain and temperature through Brillouin frequency shift," *IEEE Photonics Technol. Lett.* **13**, 1094–1096 (2001).
- ¹²W. Zou, Z. He, and K. Hotate, "Complete discrimination of strain and temperature using Brillouin frequency shift and birefringence in a polarization-maintaining fiber," *Opt. Express* **17**, 1248–1255 (2009).
- ¹³Y. Mizuno, N. Hayashi, H. Tanaka, Y. Wada, and K. Nakamura, "Brillouin scattering in multi-core optical fibers for sensing applications," *Sci. Rep.* **5**, 11388 (2015).
- ¹⁴M. A. S. Zaghoul, M. Wang, G. Milione, M.-J. Li, S. Li, Y.-K. Huang, T. Wang, and K. P. Chen, "Discrimination of Temperature and Strain in Brillouin Optical Time Domain Analysis Using a Multicore Optical Fiber," *Sensors* **18**, 1176 (2018).
- ¹⁵P. Dragic, T. Hawkins, P. Foy, S. Morris, and J. Ballato, "Sapphire-derived all-glass optical fibres," *Nat. Photonics* **6**, 627–633 (2012).
- ¹⁶P. D. Dragic, M. G. Pamato, V. Iordache, J. D. Bass, C. J. Kucera, M. Jones, T. W. Hawkins, and J. Ballato, "Athermal distributed Brillouin sensors utilizing all-glass optical fibers fabricated from rare earth garnets: LuAG," *New J. Phys.* **18**, 015004 (2015).
- ¹⁷X. Lu, M. A. Soto, and L. Thévenaz, "Temperature-strain discrimination in distributed optical fiber sensing using phase-sensitive optical time-domain reflectometry," *Opt. Express* **25**, 16059–16071 (2017).
- ¹⁸C. Xing, C. Ke, Z. Guo, K. Yang, H. Wang, Y. Zhong, and D. Liu, "Distributed multi-parameter sensing utilizing Brillouin frequency shifts contributed by multiple acoustic modes in SSMF," *Opt. Express* **26**, 28793–28807 (2018).
- ¹⁹M. Deroh, B. Kibler, H. Maillotte, T. Sylvestre, and J.-C. Beugnot, "Large Brillouin gain in Germanium-doped core optical fibers up to a 98 mol% doping level," *Opt. Lett.* **43**, 4005–4008 (2018).
- ²⁰E. M. Dianov and V. M. Mashinsky, "Germania-Based Core Optical Fibers," *J. Light. Technol.* **23**, 3500 (2005).
- ²¹A. Wada, S. Okude, T. Sakai, and R. Yamauchi, "GeO₂ concentration dependence of nonlinear refractive index coefficients of silica-based optical fibers," *Electron. Commun. Jpn. Part Commun.* **79**, 12–19 (1996).
- ²²C. Maxime, K. Courtney, H. Thomas, D. Jay, P. Dragic, and J. Ballato, "A unified materials approach to mitigating optical nonlinearities in optical fiber. III. Canonical examples and materials road map," *Int. J. Appl. Glass Sci.* **9**, 447–470 (2017).
- ²³M. Nikès, L. Thévenaz, and P. A. Robert, "Brillouin gain spectrum characterization in single-mode optical fibers," *J. Light. Technol.* **15**, 1842–1851

- (1997).
- ²⁴W. Zou, Z. He, and K. Hotate, "Investigation of Strain- and Temperature-Dependences of Brillouin Frequency Shifts in GeO₂-Doped Optical Fibers," *J. Light. Technol.* **26**, 1854–1861 (2008).
- ²⁵J.-C. Beugnot, T. Sylvestre, D. Alasia, H. Maillotte, V. Laude, A. Monteville, L. Provino, N. Traynor, S. F. Mafang, and L. Thévenaz, "Complete experimental characterization of stimulated Brillouin scattering in photonic crystal fiber," *Opt. Express* **15**, 15517–15522 (2007).
- ²⁶G. P. Agrawal, *Nonlinear Fiber Optics* (Academic Press, 2007).
- ²⁷J. Cheng-Kuei, N. Christian, S. Alain, A. Koich, B. Lee, and K. Junichi, "Acoustic Characterization of Silica Glasses," *J. Am. Ceram. Soc.* **76**, 712–716 (1993).
- ²⁸S. R. Kawa and S.-J. Lin, "Longitudinal acoustic modes and Brillouin-gain spectra for GeO₂-doped-core single-mode fibers," *JOSA B* **6**, 1167–1174 (1989).
- ²⁹X. Lu, M. A. Soto, and L. Thévenaz, "Impact of the Fiber Coating on the Temperature Response of Distributed Optical Fiber Sensors at Cryogenic Ranges," *J. Light. Technol.* **36**, 961–967 (2018).
- ³⁰T. Kurashima, T. Horiguchi, and M. Tateda, "Thermal effects on the Brillouin frequency shift in jacketed optical silica fibers," *Appl. Opt.* **29**, 2219–2222 (1990).
- ³¹P. D. Dragic, C. Ryan, C. J. Kucera, M. Cavillon, M. Tuggle, M. Jones, T. W. Hawkins, A. D. Yablon, R. Stolen, and J. Ballato, "Single- and few-mode lithium aluminosilicate optical fiber for athermal Brillouin strain sensing," *Opt. Lett.* **40**, 5030–5033 (2015).
- ³²X. Feng, C. Sun, X. Zhang, and F. Ansari, "Determination of the coefficient of thermal expansion with embedded long-gauge fiber optic sensors," *Measurement Science and Technology* **21**, 065302 (2010).